Applied Physics Letters

Multiple-sound-source-excitation quartz-enhanced photoacoustic spectroscopy based on a single-line spot pattern multi-pass cell

Cite as: Appl. Phys. Lett. **118**, 161101 (2021); https://doi.org/10.1063/5.0047963
Submitted: 17 February 2021 . Accepted: 02 April 2021 . Published Online: 19 April 2021

Ruyue Cui, Hongpeng Wu, Lei Dong, Weidong Chen, and Frank K. Tittel

AIP Publishing

Applied Physics Letters ARTICLE scitation.org/journal/apl

Multiple-sound-source-excitation quartz-enhanced photoacoustic spectroscopy based on a single-line spot pattern multi-pass cell

Cite as: Appl. Phys. Lett. **118**, 161101 (2021); doi: 10.1063/5.0047963
Submitted: 17 February 2021 · Accepted: 2 April 2021 ·
Published Online: 19 April 2021

View Online Export Citation CrossMark

Ruyue Cui,[1,2,3] Hongpeng Wu,[1,2] Lei Dong,[1,2,a)] Weidong Chen,[3] and Frank K. Tittel[4]

AFFILIATIONS

[1]State Key Laboratory of Quantum Optics and Quantum Optics Devices, Institute of Laser Spectroscopy, Shanxi University, Taiyuan 030006, China
[2]Collaborative Innovation Center of Extreme Optics, Shanxi University, Taiyuan 030006, China
[3]Laboratoire de Physicochimie de l'Atmosphère, Université du Littoral Côte d'Opale, Dunkerque 59140, France
[4]Department of Electrical and Computer Engineering, Rice University, 6100 Main Street, Houston, Texas 77005, USA

[a)]Author to whom correspondence should be addressed: donglei@sxu.edu.cn

ABSTRACT

Multiple-sound-source-excitation quartz-enhanced photoacoustic spectroscopy (MSSE-QEPAS) based on a single-line spot pattern multi-pass cell (MPC) is reported for trace gas detection. The single-line spot pattern MPC is designed to make a laser beam pass through a quartz tuning fork (QTF) 60 times, thus producing 60 sound sources between the two QTF prongs. These sound sources excite the QTF operating at fundamental resonance mode in phase, resulting in a signal gain factor of ~20. A theoretical mode based on convolution method is proposed to explain the working mechanism of MSSE-QEPAS.

Optical sensing of trace gas based on laser absorption spectroscopy has been widely used in many fields such as atmospheric monitoring, medical diagnosis, and industrial process control due to its unique advantages including high selectivity and sensitivity, on-line and real-time monitoring without any sample preparation.[1–6] Several laser-based methods, such as tunable diode laser absorption spectroscopy (TDLAS),[7] cavity-enhanced absorption spectroscopy (CEAS),[8] quartz-enhanced photoacoustic spectroscopy (QEPAS),[9,10] etc., have been developed for trace gas detection, leading to the advent of reliable and robust sensors.[11–13] In these gas detection techniques, QEPAS is an attractive approach characterized by high cost effectiveness, high sensitivity, and small footprint,[14,15] since a high *Q*-factor, low-cost quartz tuning fork (QTF) is used as the acoustic detector.

In QEPAS, a modulated laser beam is focused through a QTF gap. When the laser beam interacts with target analyte around the QTF, an acoustic point source is generated between two QTF prongs, forcing the QTF prongs to oscillate back and forth. In this way, the in-plane anti-symmetrical vibration of the QTF is excited.[16] As a result, the QTF can be treated as an acoustic quadrupole, providing good immunity to external (outside between two prongs) environmental sound.[17,18] Actually, an outgoing cylindrically symmetric pressure wave is produced along all the laser transmission paths, not just between two prongs. But the thickness of an ordinary QTF is <0.4 mm, which means that only the sound wave from the QTF-thickness-long sound source is effectively picked up. If the more sound waves along the beam path can be collected, the QEPAS signal can be significantly improved.

As the QTF thickness is limited by the its geometry design and manufacturing process, an alternative approach is to fold the laser beam, making it pass through the QTF repeatedly and thus yielding multiple sound sources between two QTF prongs. All the sound waves from these sound sources together drive two QTF prongs to vibrate, hence enhancing signal amplitude. In 2017, a quartz-enhanced photoacoustic spectrophone driven by two acoustic point sources was demonstrated, in which a laser beam passed through the QTF two times by means of a mirror and an optical circulator, producing two acoustic point sources along the QTF symmetry axis and successfully exciting the two resonance antinodes of the QTF operating at an 1st overtone resonance mode.[19] Finally, a signal gain factor of 3 was achieved. However, the phases of the laser beams at the two antinodes must meet a specific phase relationship, which requires an additional phase control system, resulting in a complicated equipment.

In fact, a multi-pass cell (MPC) composed of two high reflectivity spherical or aspherical mirrors is a powerful tool to increase the number of a beam reflections.[20] However, a big challenge is to make all these back-and-forth laser beams between two mirrors fall on a plane, so that all of the beams can pass through the narrow QTF gap between two prongs. In 2020, a spherical aberration-based theoretical model of two-spherical-mirror MPCs was developed by Dong *et al.*,[21,22] which can generate exotic spots patterns under a careful design, thus paving a way for the combination of MPC and QTF.

In this Letter, multiple-sound-source-excitation quartz-enhanced photoacoustic spectroscopy (MSSE-QEPAS) is reported, in which a photoacoustic combination of a QTF and a MPC is demonstrated. The MPC designed based on spherical aberration has a single-line spot pattern on its two mirrors, which implies that all laser beams between two mirrors fall on one plane. A custom QTF with a large prong spacing is inserted into the MPC. The laser beams pass through the QTF's gap repeatedly, producing multiple acoustic point sources along the QTF symmetry axis. As a result, the QTF operating at a fundamental resonance mode is simultaneously excited by the multiple acoustic point sources and effectively collects the more sound waves to enhance the signal output.

In MSSE-QEPAS, the design of the MPC should follow the below rules: (1) all laser beams must fall on one plane in order to pass through a QTF gap, (2) all light spots on the mirrors should be concentrated within a short single-line segment due to the limited prong length of a QTF, (3) the more beam reflections are desirable to increase the number of sound sources between two prongs, and (4) spot overlaps are allowed which can increase the radiation intensity of the sound source generated by the overlapping spots. In order to obtain an optimal MPC with a single-line spot pattern, a large number of numerical calculations were carried out using the theoretical model of spherical aberration with a variety of initial parameters. The diameter and the curvature radius of the used spherical mirror were fixed to 10 mm and 100 mm, respectively. This incident location of the laser beam on the input mirror was (0, 6.25 mm). The incident beam diameter was set as 0.6 mm. When the mirror spacing was 36.6 mm and the incident angle of the initial beam was $\sim 5°$, a single-line spot pattern was achieved, as shown in Fig. 1(a). Moreover, the spot distribution between two prongs of the QTF can be simulated by use of the Irradiance Map in TracePro, as shown in Fig. 1(b). Although spot overlaps usually cause etalon effect in TDLAS, MSSE-QEPAS as a zero-background technique does not pick up the etalon noise since it detects sound rather than light. The single-line spot pattern in Fig. 1 can provide 60 pass counts and the projected area on the x-y plane is less than $\sim 8\ \mathrm{mm}^2$.

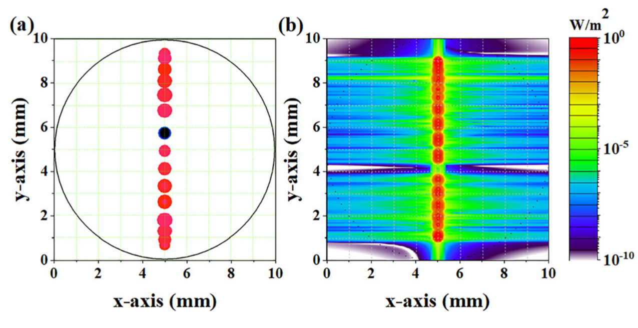

FIG. 1. (a) Single-line spot pattern generated by a theoretical model of two-spherical-mirror MPCs based on spherical aberration. The plot represents the spot projection of the incident mirror. Black spot represents the coincident incident and exit positions of beams. (b) Simulation of spot distribution on the symmetry plane between two mirrors using TracePro. The spot size stands for irradiance.

The schematic diagram of a MSSE-QEPAS sensor system is depicted in Fig. 2. A custom QTF with a resonance frequency of $f_0 = 7.2057$ kHz was employed, which had a prong length and spacing of 10 mm and 800 μm, respectively. Such a prong spacing ensures all the ray trajectories in this MPC to fall within the QTF's gap without the light-induced photoacoustic thermal noise.[23] The Q factor of the QTF was measured to be 6020. The custom QTF was inserted into the center of the designed MPC. A photograph was shown in the inset of Fig. 2. A continuous wave (CW) fiber-coupled distributed feedback (DFB) laser with a wavelength of 1.395 μm and output power of 16 mW was used as a probe light source. A custom laser control circuit board (CCB) was used to control the driving current and laser temperature by means of a laptop. To improve the performance of the MSSE-QEPAS sensor, wavelength modulation technique was implemented. A ramp signal generated from the laptop scans the laser wavelength across the absorption line. A sine wave signal modulates the laser wavelength at a frequency of $f_0/2$. The DFB laser was connected to a fiber collimator with a $\sim 600\ \mu$m beam waist at a working distance of 80 mm. The laser beam was coupled into the designed MPC. The collimator was placed 80 mm away from the QTF; thus, the laser beam waist was located at the center of the MPC. The output electrical signal from the custom QTF was connected to a low-noise transimpedance amplifier and then transferred to a commercial lock-in amplifier (Stanford Research Systems, Model SR830). The lock-in amplifier demodulated the signal in the 2f mode with respect to the sync signal. The lock-in amplifier was set to a 12 dB/oct filter slope and a time constant $\tau = 1$ s corresponding to a detection bandwidth of 0.25 Hz. The demodulation signal of 2f spectra was delivered to the laptop for analysis and display.

Performances of the MSSE-QEPAS sensor system were optimized by detecting the fixed concentration of water vapor at atmospheric pressure and room temperature. A commercial dew point hygrometer was used to calibrate the concentration of water vapor. The selected H_2O target line is located at 7181 cm^{-1}. Since the QEPAS signal strongly depends on the position of the laser focusing point

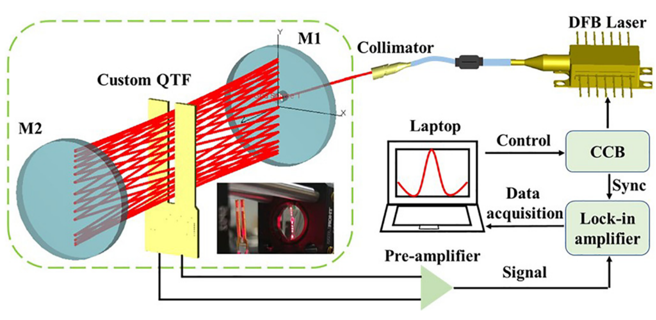

FIG. 2. MSSE-QEPAS system configuration. Red lines: transmission of the laser beams between two identical spherical mirrors, M1 and M2; QTF: quartz tuning fork; CCB: control circuit board. Inset: Photograph of the single-line spot pattern on the M1 surface and the QTF.

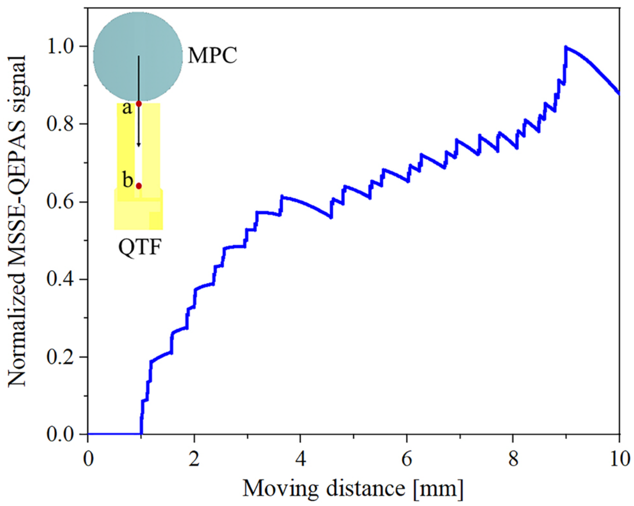

FIG. 3. Normalized MSSE-QEPAS signal amplitudes as a function of the vertical moving distance of the MPC.

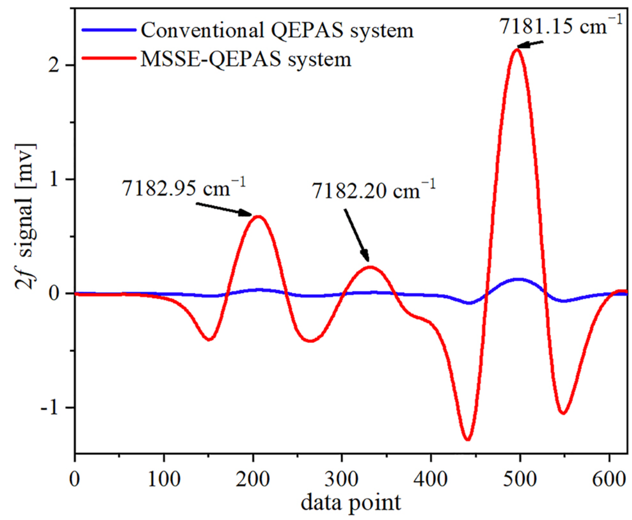

FIG. 4. $2f$ signals of conventional QEPAS system (blue line) and MSSE-QEPAS system (red line).

along the QTF axis,[24] the depth of the QTF into the MPC has to be optimized according to the output signal. A 3-dimensional linear stage with a typical step size of 1 μm was used to move the MPC from the top (point a) to the bottom (point b) along the QTF symmetry axis, as shown in Fig. 3. The normalized MSSE-QEPAS signal amplitudes were also plotted in Fig. 3 as a function of the vertical moving distance of the MPC. Due to the fact there were no beams from 0 to 1 mm on the symmetry axis of Fig. 1(b), the MSSE-QEPAS peak signal was $\sim$0 in the moving distance of 0–1 mm. The highest signal amplitude was achieved when the moving distance is $\sim$9 mm. A significant increase in the signal was not observed when the QTF was moved left and right along the optical axis of this MPC.

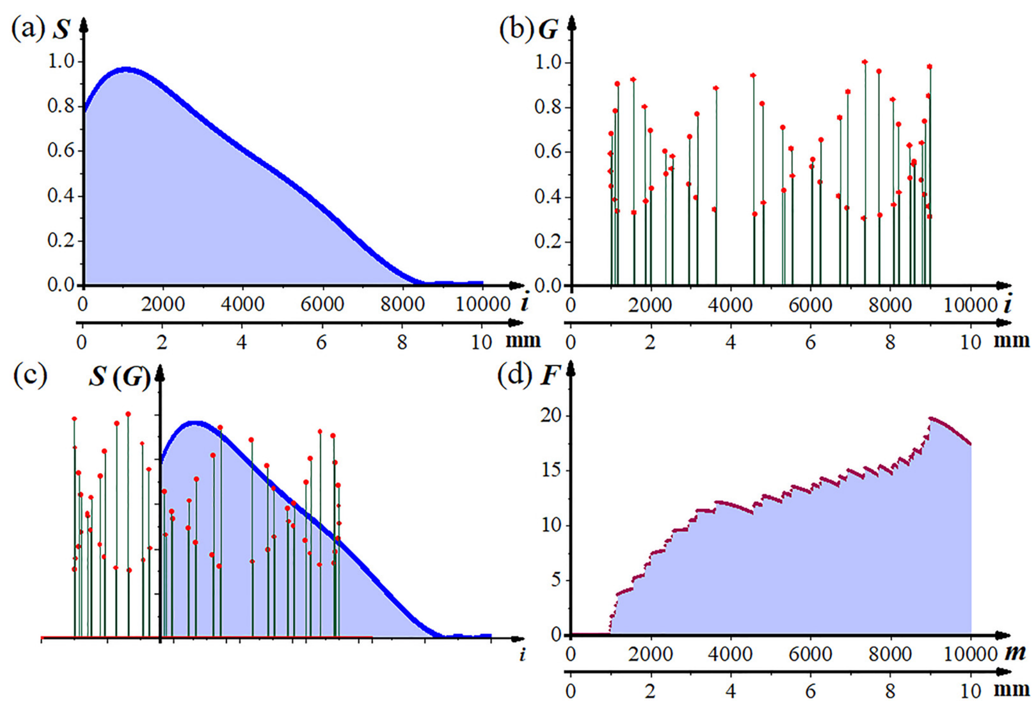

FIG. 5. (a) Normalized traditional QEPAS signals measured by changing the position of the excitation light from the top to the bottom of QTF. (b) 60 laser beam normalized intensities and distribution along i. (c) Calculation process of the convolution model. (d) Signal amplitudes of MSSE-QEPAS at different QTF insertion depths.

The signal gain factor of the MSSE-QEPAS sensor system at the optimal moving distance of 9 mm was assessed. The $2f$ signal peak was measured to be 2.14 mV with an 8500-ppm H_2O/N_2, as shown in Fig. 4. In order to compare with traditional QEPAS, the MPC was removed from the sensor system, enabling the laser beam pass through the QTF once. The QEPAS signal amplitudes were scanned from the top (point a) to the bottom (point b) along the QTF symmetry axis under the same conditions, as recorded in Fig. 5(a). The highest signal amplitude was 112.5 μV, which was observed at $\sim$1.2 mm. The optimal position is consistent with the previous result.[25] Therefore, the signal gain factor of MSSE-QEPAS is 19 with respect to traditional QEPAS, as shown in Fig. 4.

The used MPC provides 60 light beam pass counts. An anticipated signal gain factor should be $\sim$60 if a linear enhancement mechanism was taken into account. However, the actual signal gain factor is three times less than the anticipated value. Here, we proposed a theoretical model to understand the behavior. $S[i]$ is defined as the traditional QEPAS signals as shown in Fig. 5(a), the maximum of which at $\sim$1.2 mm was normalized to unit 1. The variable i is the QTF symmetry axis. It is discretized for the convenience of the numerical calculation and is an integer, one of which stands for a typical 1-μm step size of the 3-dimensional linear stage. $G[i]$ is defined as the laser beam intensity, which is equal to $\mathrm{R}^{\mathrm{n}(i)}$ $[0 \le \mathrm{n} \le 59]$ or 0 depending on if there is or isn't a laser beam at i. Here, $\mathrm{R} = 0.98$ is the mirror reflectivity of the MPC, and $\mathrm{n}(i)$ is the number of the beam reflections at i. The first laser beam intensity without any reflections ($\mathrm{n} = 0$) is unit 1. The 60 laser beam intensities between two QTF prongs as a function of i are shown in Fig. 5(b). In fact, the process of a QTF inserting into a MPC can be described as a convolution operation,

$$F[m] = S[m] * G[m] = \sum_{i=-\infty}^{\infty} S[i]G[m-i], \tag{1}$$

where m is the moving distance and $F[m]$ is the signal amplitudes of MSSE-QEPAS at different QTF insertion depths. The calculation process and the result of the convolution are shown in Figs. 5(c) and 5(d), respectively. The ladder pattern of $F[m]$ is attributed to the distribution of the discrete laser intensity $G[i]$. The maximum signal amplitude of 19.8 was achieved at $m = 8988$, which corresponds to the moving distance of $\sim$9 mm. Considering the normalized QEPAS signal amplitude at Fig. 5(a), the calculated signal gain factor is 19.8, which is in excellent agreement with the experimental results.

In conclusion, we realized a QEPAS sensor excited by 60 sound sources by use of a single-line pattern MPC and a QTF operating at the fundamental resonance mode. Unlike the 1st overtone resonance mode reported previously, all sound waves from the 60 sound sources contributed to the in-phase prong deflections of the QTF without any phase shift, producing a signal gain factor of $\sim$20. Highly sensitive QEPAS sensors based on MSSE-QEPAS described in this Letter have many uses in atmospheric monitoring, industry process control, and medical diagnostics. Further topics of interest include reducing the mirror size according to the single-line spot pattern and increasing the pass count of the light in the MPC, as well as concentrating all the beams within the highly sensitive top part of a QTF.

AUTHORS' CONTRIBUTIONS

R.C. and H.W. contributed equally to this work.

The project is sponsored by National Key R&D Program of China (No. 2019YFE0118200), National Natural Science Foundation of China (NSFC) (Nos. 62075119 and 61805132), Sanjin Scholar (No. 2017QNSJXZ-04), and Shanxi "1331KSC." Frank K. Tittel acknowledges the support by the Robert Welch Foundation (Grant No. C0586).

DATA AVAILABILITY

The data that support the findings of this study are available from the corresponding author upon reasonable request.

REFERENCES

[1] L. Dong, C. Li, N. P. Sanchez, A. K. Gluszek, R. J. Griffin, and F. K. Tittel, Appl. Phys. Lett. **108**, 011106 (2016).
[2] A. A. Kosterev, Y. A. Bakhirkin, F. K. Tittel, S. Mcwhorter, and B. Ashcraft, Appl. Phys. B **92**, 103–109 (2008).
[3] W. Ren, L. Q. Luo, and F. K. Tittel, Sens. Actuator, B **221**, 1062 (2015).
[4] H. Wu, L. Dong, X. Yin, A. Sampaolo, P. Patimisco, W. Ma, L. Zhang, W. Yin, L. Xiao, V. Spagnolo, and S. Jia, Sens. Actuators, B **297**, 126753 (2019).
[5] X. Yin, H. Wu, L. Dong, B. Li, W. Ma, L. Zhang, W. Yin, L. Xiao, S. Jia, and F. K. Tittel, ACS Sens. **5**, 549–556 (2020).
[6] H. Zheng, L. Dong, H. P. Wu, X. K. Yin, L. T. Xiao, S. Jia, R. F. Curl, and F. K. Tittel, Chem. Phys. Lett. **691**, 462–472 (2018).
[7] R. Cui, L. Dong, H. Wu, W. Ma, W. Yin, and F. K. Tittel, Anal. Chem. **92**, 13034–13041 (2020).
[8] Q. He, C. Zheng, M. Lou, W. Ye, Y. Wang, and F. K. Tittel, Laser Phys. **26**(12), 15436–15444 (2018).
[9] L. Dong, A. A. Kosterev, D. Thomazy, and F. K. Tittel, Appl. Phys. B **100**, 627–635 (2010).
[10] Y. Ma, Appl. Sci. **8**, 1822 (2018).
[11] S. Qiao, Y. Ma, P. Patimisco, A. Sampaolo, Y. He, Z. Lang, F. K. Tittel, and V. Spagnolo, Opt. Lett. **46**, 977 (2021).
[12] R. Cui, L. Dong, H. Wu, S. Li, L. Zhang, W. Ma, W. Yin, L. Xiao, S. Jia, and F. K. Tittel, Opt. Express **26**, 24318 (2018).
[13] S. Borri, P. Patimisco, I. Galli, D. Mazzotti, G. Giusfredi, N. Akikusa, M. Yamanishi, G. Scamarcio, P. De Natale, and V. Spagnolo, Appl. Phys. Lett. **104**, 091114 (2014).
[14] P. Patimisco, A. Sampaolo, L. Dong, F. K. Tittel, and V. Spagnolo, Appl. Phys. Rev. **5**, 011106 (2018).
[15] H. Wu, L. Dong, H. Zheng, Y. Yu, W. Ma, L. Zhang, W. Yin, L. Xiao, S. Jia, and F. K. Tittel, Nat. Commun. **8**, 15331 (2017).
[16] N. Petra, J. Zweck, A. A. Kosterev, S. E. Minkoff, and D. Thomazy, Appl. Phys. B **94**, 673–680 (2009).
[17] Y. F. Ma, S. D. Qiao, P. Patimisco, A. Sampaolo, Y. Wang, F. K. Tittel, and V. Spagnolo, Appl. Phys. Lett. **116**, 061101 (2020).
[18] Z. L. Li, Z. Wang, Y. Qi, W. Jin, and W. Ren, Sens. Actuators, B **248**, 1023 (2017).
[19] H. Zheng, L. Dong, P. Patimisco, H. Wu, A. Sampaolo, X. Yin, S. Li, W. Ma, L. Zhang, W. Yin, L. Xiao, V. Spagnolo, S. Jia, and F. K. Tittel, Appl. Phys. Lett. **110**, 021110 (2017).
[20] D. Herriott, H. Kogelnik, and R. Kompfner, Appl. Opt. **3**, 523 (1964).
[21] R. Cui, L. Dong, H. Wu, S. Li, X. Yin, L. Zhang, W. Ma, W. Yin, and F. K. Tittel, Opt. Lett. **44**(5), 1108 (2019).
[22] R. Cui, L. Dong, H. Wu, W. Chen, and F. K. Tittel, Appl. Phys. Lett. **116**, 091103 (2020).
[23] V. Spagnolo, P. Patimisco, S. Borri, G. Scamarcio, B. E. Bernacki, and J. Kriesel, Appl. Phys. B **112**, 25–33 (2013).
[24] P. Patimisco, G. Scamarcio, F. K. Tittel, and V. Spagnolo, Sensors **14**, 6165–6206 (2014).
[25] H. Wu, A. Sampaolo, L. Dong, P. Patimisco, X. Liu, H. Zheng, X. Yin, W. Ma, L. Zhang, W. Yin, V. Spagnolo, S. Jia, and F. K. Tittel, Appl. Phys. Lett. **107**, 111104 (2015).